STUDIA UNIV. "BABEŞ–BOLYAI", MATHEMATICA, Volume **XLIX**, Number 4, December 2004

PERIODIC AND QUASIPERIODIC MOTION IN THE PERIODICALLY FORCED RAYLEIGH SYSTEM

PETRE BĂZĂVAN

Abstract. In this paper we present a numerical study of the periodic and quasiperiodic motion in the dynamical system associated with the generalized Rayleigh equation. Numerical results describe the system dynamics changes (in particular bifurcations), when the forcing amplitude is varied.

1. Introduction

The autonomous second order nonlinear ordinary differential equation (ODE),

$$\ddot{x} + \frac{\dot{x}^3}{3} - \dot{x} + x = 0, \tag{1}$$

introduced in 1883 by Lord Rayleigh, is the nonlinear equation which appears to be the closest to the ODE of the harmonic oscillator with dumping [1]. Some aspects concerning *canard* bifurcations are analyzed in [1] and [2] for the periodically forced generalization of Rayleigh equation,

$$\varepsilon\ddot{x} + \frac{\dot{x}^3}{3} - \dot{x} + ax = g\sin\omega t. \tag{2}$$

From mathematical perspective the nonautonomous system of nonlinear ODEs associated with (2) is one of a class of periodically forced nonlinear oscillators, as the Van der Pol and Bonhoeffer Van der Pol systems are.

The behavior of these systems was much numerically investigated in [3], [4] and [14], due to their applications in electronics and physiology.

Received by the editors: 22.04.2004.

2000 *Mathematics Subject Classification.* 34K28, 37C50, 37C70, 37G15, 37M20.

Key words and phrases. Bifurcations, periodic and quasiperiodic motion, Poincaré map, Lyapunov exponents, attractors.

With system (2) there are associated the two-dimensional nonlinear non-autonomous system of ODEs

$$\begin{cases} \dot{x}_1 = x_2, \\ \dot{x}_2 = -\frac{a}{\varepsilon}x_1 + \frac{1}{\varepsilon}x_2 - \frac{x_2^3}{3} + g\sin\omega t, \end{cases} \tag{3}$$

and the three-dimensional nonlinear autonomous system

$$\begin{cases} \dot{x}_1 = x_2, \\ \dot{x}_2 = -\frac{a}{\varepsilon}x_1 + \frac{1}{\varepsilon}\left(x_2 - \frac{x_2^3}{3}\right) + \frac{g}{\varepsilon}\sin x_3, \\ \dot{x}_3 = \omega \, mod \, 2\pi. \end{cases} \tag{4}$$

A three-dimensional dynamical system with the phase space $\mathbb{R}^2 \times S^1$ can be associated with (4).

Periodic solutions and the dynamics of the systems associated with (3) and (4) are studied in [6] and [7]. The succession of the periodic and chaotic attractors for the system (4) and then, the transition between the periodic and chaotic motion are numerically studied in [8].

The dynamical system associated with (4) involves the interaction between two periodic motions, each with a different frequency. When the ratio of the frequencies is irrational the dynamical system behaves in a manner which is neither periodic or chaotic. This motion is called *quasiperiodic*. More precisely, the natural periodic motion, studied in [6] for the unforced case, i.e. Eq. (1), is modulated by a second periodic motion given by the sinusoidal term when $g > 0$. The system behaves in a manner with the motion never quite repeating any previous motion. This behavior is generically followed by the system locking into a periodic motion, as the control parameter for the system is varied [14].

The aim of our numerical analysis is to establish the parameter region where the system (4) presents a quasiperiodic motion and structural changes which may lead to any subsequent mode locked region of periodic motion.

The mathematical model used in our numerical study is presented in Sec. 2. Numerical results in Sec. 3 are concerned with the proof of the existence of the

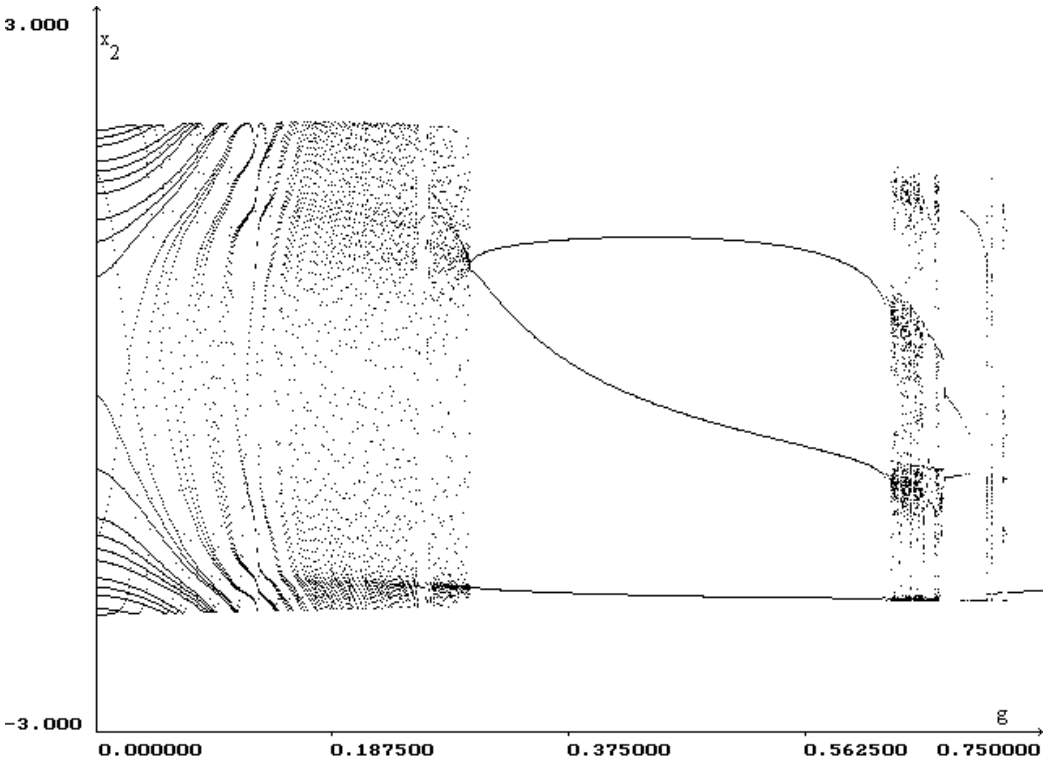

FIGURE 1. Bifurcation diagram for the dynamical system (4).

quasiperiodic motion and the study of the transition from quasiperiodic to periodic motion in the system (4).

2. **The mathematical model**

In order to present the mathematical model used in the numerical study from Sec. 3, we shortly write (4) in the form

$$\dot{x}= f\left(x\right), \tag{5}$$

where f is defined on the $\mathbb{R}^2 \times S^1$ cylinder. We define a Poincaré map as follows. Let

$$\sum = \left\{ (x_1, x_2, x_3) \in \mathbb{R}^2 \times S^1, x_3 = 0 mod \frac{2\pi}{\omega} \right\}$$

be a surface of section, which is transversally crossed by the orbits of (5). The Poincaré map $P : \Sigma \to \Sigma$ is defined by

$$P(x_0) = x(2\pi/\omega, x_0) = \int_0^{2\pi/\omega} f(x(t, x_0))\, dt \tag{6}$$

where $x_0 \in \Sigma$ and $x(t, x_0)$ is the solution of the Cauchy problem $x(0) = x_0$ for (5). We denote by P^n the n-times iterated map.

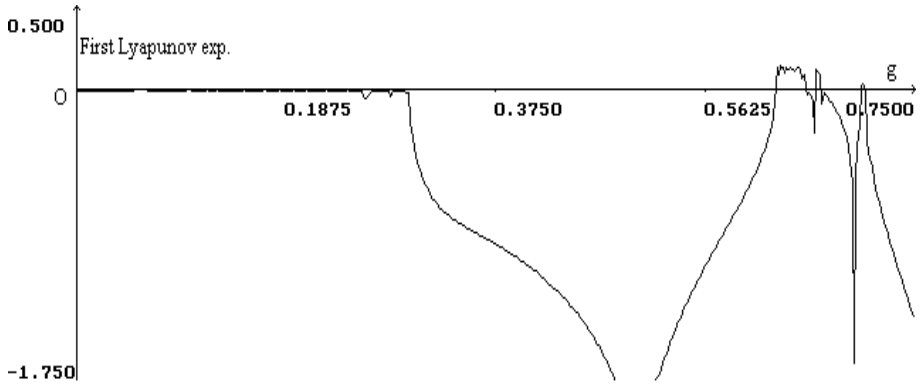

FIGURE 2. The first Lyapunov exponent for the dynamical system (4).

Let be $\xi(t, x_0)$ a periodic solution of (5) with period $T = n \cdot 2\pi/\omega$, $n \geq 1$, lying on a closed orbit and consider the map P of the initial point x_0. Then, to this closed orbit an n-periodic orbit of P corresponds. Numerically, the period T (i.e. n from the expression of T) can be determined by integrating Eq. (5) with the initial condition x_0 and sampling the orbit points $x_k = P(x_{k-1})$, $k \geq 1$ at discrete times $t_k = k \cdot 2\pi/\omega$, until $P^k(x_0) = x_0$. Then, $n = k$.

The stability discussion of the periodic orbit $\xi(t, x_0)$ is reduced to the stability discussion of the fixed point x_0 of P^n since the stability of the periodic solution ξ is determined by the eigenvalues of the matrix DP^n, [9], [10], [11]. The linear stability of the n-periodic orbit of P is determined from the linearized-map matrix DP^n of P^n. The matrix DP^n can be obtained by integrating the linearized system (5) for a small perturbation $y \in \mathbb{R}^2 \times S^1$, [9], [10]. We note [9] that one of the eigenvalues of this matrix always equals 1, and that the remained two eigenvalues, also called the

Poincaré map multipliers, influence the stability. We denote these eigenvalues by λ_1 and λ_2.

The diagnostics used to establish structural changes of the system (4) involve two-dimensional $x_1 - x_2$ phase plane diagrams, Poincaré sections at intervals of forcing period $2\pi/\omega$, bifurcation diagrams with $g - x_2$ coordinates, evaluations of the eigenvalues of the linearized Poincaré map-matrix, evaluations of the Lyapunov exponents.

All numerical calculations were carried out through the application of a variable step-size algorithm for Runge-Kutta methods [12], [13]. This algorithm is a variant of an algorithm [14], [15] which controls the time step with a Richardson extrapolation method [16]. For the calculation of Lyapunov exponents we used the method described in [17]. The 3D-representation uses a center projection [18].

3. **Periodic and quasiperiodic motion**

In our numerical study we investigated a region in the four-dimensional parameter space $(\varepsilon, a, g, \omega)$ given by $0 < \varepsilon \leq 1$, $0 < a \leq 1$, $1 < \omega \leq 3$ and $0 < g \leq 2$. By logistic reasons we restrict the presentation to the region space

$$\varepsilon = 0.125, \qquad a = 0.5, \qquad \omega = 2.84, \qquad 0 < g \leq 0.75. \tag{7}$$

An overview of the numerical results which typify the system is given by the bifurcation diagram in Fig. 1.

In the first part of the subinterval $0 < g < 0.3$ we observe an apparent regularity of the return points. This region which can indicate a quasiperiodic or chaotic behavior is followed by a region with clear periodic motion. This last region is interrupted by short chaotic regions. We prove the existence of the quasiperiodic behavior in two ways.

The first argument is the first Lyapunov exponent value. Recall that a leading Lyapunov exponent of zero verifies quasiperiodic behavior [14]. Fig. 2 is a graph of the control parameter (the forcing amplitude g) against the first Lyapunov exponent for the same parameter range as the bifurcation diagram of Fig. 1. In the interval

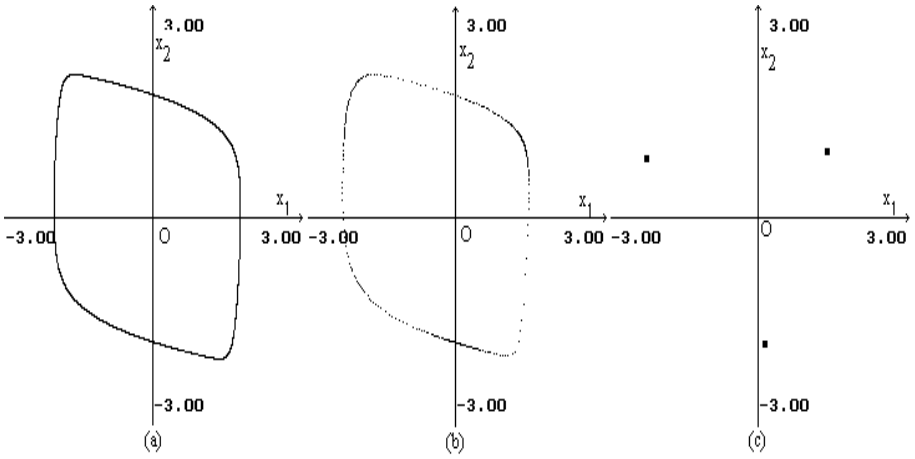

FIGURE 3. Poincaré sections for the dynamical system (4).

$0 < g < 0.3$ the exponent was consistently within -0.01 of 0. This is the first numerical confirmation of the quasiperiodic behavior.

The intersection points of the trajectories of the system (4) with the associated Poincaré section represent the second argument. At $g_1 = 0.07$ the section is represented in the Fig. 3a. The drift ring is associated with quasiperiodic motion. Integrating with a large period, the curve does not modify the shape. The fact that the points are situated on a closed curve and the constant shape related to the integration time confirm the quasiperiodic behavior [14].

In proportion as g increases in the interval $0 < g < 0.3$ the return points remain on the same curve but the density increases markedly in some locations (Fig. 3b for $g_2 = 0.25$). At $g_3 = 0.3$ there are only three intersection points in the Poincaré section (Fig. 3c) and on the bifurcation diagram the quasiperiodic region is replaced by a periodic window. The motion changes from quasiperiodic to periodic, with the emergence of a period-3 attractor. This is due to the saddle-node bifurcation of the Poincaré map P^3,

$$x_{n+3} = P^3(x_n), \quad x_0 \in \mathbb{R}^2 \times S^1, \quad n \geq 0.$$

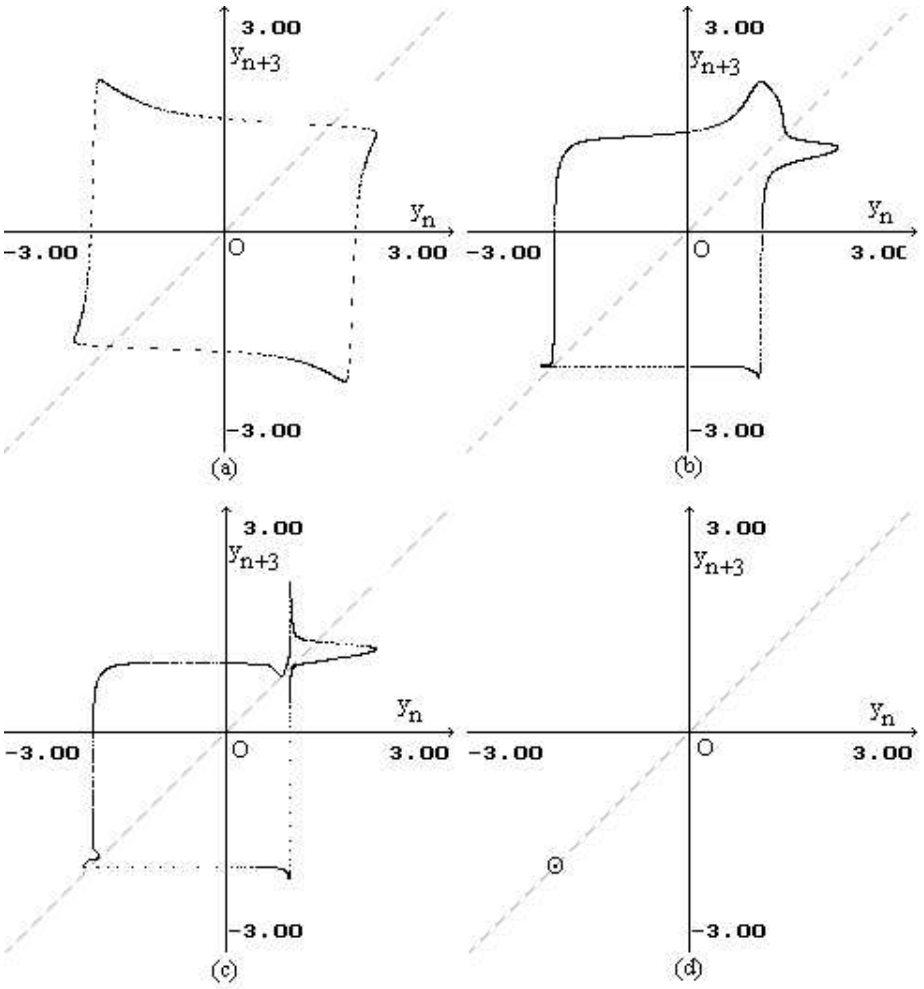

FIGURE 4. The Poincaré map P^3 associated with the dynamical system (4).

We numerically prove this fact. We use the projection of the graph of P^3 on the plane (y_n, y_{n+3}), $n \geq 0$, where we denote by y the x_2 coordinate of the point $x \in \mathbb{R}^2 \times S^1$.

In Fig. 4a for $g_4 = 0.07$, when the motion is quasiperiodic, there are two intersection points of P^3 with the diagonal $y_n = y_{n+3}$. At the intersection the magnitude of the slope not equals 1. As g increases the curve approaches the diagonal

in other locations (Fig. 4b for $g_5 = 0.28$). These locations suggest the imminent tangential intersections. At $g_6 = 0.2961$ there are three tangential intersections (Fig. 4c) and we have a saddle-node bifurcation of the map P^3. When $g_7 = 0.3$ (Fig. 4d) the graph of the map P^3 is a single point which is situated on the diagonal. This fact confirms the existence of the period-3 attractor.

References

[1] M. Diener M., *Nessie et les canards*, IRMA, Strasbourg, 1979.

[2] M. Diener, *Quelques examples de bifurcations et les canards*, Publ. IRMA, Strasbourg, **75**/1979.

[3] I. E. Flaherty, F. C. Hoppensteadt, *Frequency entrainment of a forced Van der Pol oscillator*, Studies Appl. Math., **58**, 1978, 5-15.

[4] R. Mettin, U. Parlitz, and W. Laterborn, , *Bifurcation structure of the driven Van der Pol oscillator*, Int. J. Bifurcation and Chaos, **3**(6), 1993, 1529-1555.

[5] B. Barnes, R. Grimshow, *Numerical studies of the periodically forced Bonhoeffer Van der Pol oscillator*, Int. J. Bifurcation and Chaos, **7**(12), 1997, 2653-2689.

[6] M. Sterpu, P. Băzăvan, *Study on a Rayleigh equation*, Bul. Şt. Univ. Piteşti, Ser. Matematică-Informatică, **3**(1999), 429-434.

[7] M. Sterpu, A. Georgescu, and P. Băzăvan, *Dynamics generated by the generalized Rayleigh equation II. Periodic solutions*, Mathematical Reports, **2**(52), 2000, 367-378.

[8] P. Băzăvan, *Numerical study of the succesion of attractors in the periodicaly forced Rayleigh system*, submitted to Int. J. Bif. Chaos, 2004.

[9] P. Glendinning, *Stability, instability and chaos*, Cambridge, New York, 1995, 151-156.

[10] E. Reithmeir, *Periodic Solutions of Nonlinear Dynamical Systems*, Springer Verlag, 1991, 89-104.

[11] Y. Kuznetsov, *Elements of applied bifurcation theory*, Springer Verlag, 1998, 104-1126, 127-130, 151-156.

[12] P. Băzăvan, *A variable step-size algorithm for Runge-Kutta methods*, Roum. J. Inf. Sci. Tech., **3**(2), 2000, 105-112.

[13] P. Băzăvan, *The dynamical system generated by a variable step-size algorthm for Ruge-Kutta methods*, Int. J. Chaos Theory and Appl., **4**(4), 1999, 21-28.

[14] G. L. Baker, J. P. Gollub, Chaotic dynamics an introduction, *Cambridge University Press*, 1996, 193-195.

[15] W. H. Press, S. A. Teukolsky, W. T. Vetterling, B. P. Flannery, Numerical recipes in C: The art of scientific computing, *Cambridge University Press*, Cambridge, 1992, Cap. 16, 707-747.

[16] M. Crouziex, A. L. Mignot, Analyse numérique des équations différentielles, 2^e edition, *Masson, Paris*, 1989, 83-87, 95-104, 168-172.

[17] A. Wolf, J. B. Swift, H. L. Swinney and J. A. Vastano, Determining Lyapunov exponents ftom a time series, *Physica*, **16D**, 1985, 285-317.

[18] P. Băzăvan, *Problems of Computational Geometry in "Ray-tracing"*, Annals of Univ. of Craiova, Math.-Inf. Series, **XX**(1994), 80-88.

Department of Informatics, University of Craiova,
Al. I. Cuza Street, No. 13, Craiova RO-200585, Romania
E-mail address: bazavan@yahoo.com